Investigating dirty crossover through fidelity susceptibility and density of states

Ayan Khan

Department of Physics, Bilkent University, Bilkent 06800, Ankara, Turkey
ayankhan@fen.bilkent.edu.tr

Saurabh Basu

Department of Physics, Indian Institute of Technology-Guwahati, Guwahati, India

B. Tanatar

Department of Physics, Bilkent University, Bilkent 06800, Ankara, Turkey

We investigate the BCS–BEC crossover in an ultracold atomic gas in the presence of disorder. The disorder is incorporated in the mean-field formalism through Gaussian fluctuations. We observe evolution to an asymmetric line-shape of fidelity susceptibility (FS) as a function of interaction coupling with increasing disorder strength which may point to an impending quantum phase transition (QPT). The asymmetric line-shape is further analyzed using the statistical tools of skewness and kurtosis. We extend our analysis to density of states (DOS) for a better understanding of the crossover in the disordered environment.

Keywords: BCS–BEC crossover; fidelity susceptibility; disorder.

PACS numbers: 74.62.En, 74.20.Fg, 67.85.Lm, 64.70.Tg

1. Introduction

Atomic gases at very low temperature are unique systems where one can observe the continuous evolution of a fermionic system (BCS type) to a bosonic system (BEC type) by changing the inter-atomic interaction by means of Fano–Feshbach resonance.[1] The essence of BCS–BEC crossover rests on the two-body physics where the inter-atomic s-wave scattering length is tuned to influence the interaction from weak to strong. The weak coupling limit is characterized by the BCS theory where two fermions make a Cooper pair with a long coherence length whereas in the strong coupling limit they are closely bound to create composite bosons (short coherence length), which can undergo Bose–Einstein condensation (BEC). In this evolution

process there exists a region known as "unitarity", where the *s*-wave scattering length diverges and the interactions depend only on the inverse Fermi momentum $(1/k_F)$, which causes the physics to become independent of any length scale and therefore universal for any Fermi system. The experimental advances to realize this transition has introduced the possibility of studying the so-called BCS–BEC crossover more closely from different angles.[2–4]

The situation becomes even more interesting if one assumes the existence of random disorder in an otherwise very clean system. In the seminal work of Anderson,[5] the localization effect due to disorder was predicted for superconductors in strong disorder but the weak disorder does not produce any significant effect. It is immensely difficult to observe the localization or the exponentially decaying wavefunction in electronic systems. One usually takes the indirect route of conductivity measurements to observe the effect of localization.[6]

Ultracold atomic systems with their high level of controllability offer a chance to observe effects of disorder more directly. Recently, localization effects have been observed in Bose gases (^{87}Rb and ^{39}K).[7,8] Latest experiments are conducted for three-dimensional systems for both noninteracting atomic Fermi gas[9] of ^{40}K and Bose gas[10] of ^{87}Rb. These experiments have widened the possibility of studying the crossover in the presence of disorder[11,12] experimentally.

Recent studies on unitary Fermi gases in the presence of quenched disorder have predicted a paradigm of robust superfluidity in the crossover region[13–17] through the observation of nonmonotonic condensate fraction[13,16] and critical temperature.[15] Further, it was indicated that the weak impurity effect can lead to a quantum phase transition (QPT) by extrapolating the data of critical temperature obtained through the study of quantum fluctuations [see (Fig. 3) in Ref. 14]. These studies have motivated us to look into the BCS–BEC crossover and beyond in the presence of disorder. For this purpose we have carried out a systematic study on fidelity susceptibility (FS) and density of states (DOS) for the dirty crossover.

Recently, behavior of FS, a tool widely used in quantum computation, is successfully applied as an intrinsic criterion to study QPT and tested in a variety of models.[19–26] Since a QPT is an abrupt change of the ground state of a many-body system when a control parameter λ of the Hamiltonian crosses a critical value λ_c, it is then quite natural to expect[19] that the overlap $F(\lambda + \delta\lambda, \lambda) \equiv |\langle \Psi(\lambda + \delta\lambda) | \Psi(\lambda) \rangle|$ between the ground states corresponding to two slightly different values of the parameter λ, should manifest an abrupt drop when the small variation $\delta\lambda$ crosses λ_c. Such an overlap, which has been named "ground-state fidelity" provides a signature of a QPT. We have shown that this technique can be adequately used in the BCS–BEC crossover scenario.[27] Although BCS–BEC crossover is not a QPT, we observe a smooth nonmonotonic evolution of the FS.

In this article we study the overlap function when the system is subjected to a weak random disorder. The atom–atom interaction is modeled by a short-range (contact) potential. In Ref. 27 it was shown that for the contact potential the FS is highly symmetric and its full width at half maximum indicates the crossover

boundary. Here we observe a breakdown in symmetry (using similar short range inter-atomic interaction) with increasing disorder and we study the asymmetry by means of third and fourth moments of the FS distribution.

It is customary to analyze the electronic, topological and physical properties of different materials by a systematic study of the density-of-states DOS.[28] We note that the energy gap in DOS for BCS superconductors is same as the pairing gap for weak disorder. The energy gap shows a nonmonotonic behavior with increasing disorder strength while the pairing gap is gradually depleted. Here, we calculate the DOS in the BCS–BEC crossover region and obtain an interesting behavior at unitarity. Disorder does not introduce a significant change in DOS at the BCS and BEC regimes but a distinct drop in the energy gap at unitarity is observed.

The rest of this paper is organized as follows. In Sec. 2 we give a brief description of the disorder model and sketch of the FS calculation. We present our results and provide a general discussion in Sec. 3. We draw our conclusions in Sec. 4.

2. Formalism

In this section, we provide a sketch of the mean-field theory when subjected to static random disorder and later we review the FS calculation in the crossover picture.[27] A more comprehensive description of the disorder formalism can be found in Refs. 13, 15 and 16.

2.1. *Effect of disorder in the mean-field approximation*

To describe the effect of impurities in a Fermi superfluid evolving from BCS to BEC regimes one needs to start from the real space Hamiltonian in three-dimensions for a s-wave superfluid,

$$\mathcal{H}(\mathbf{x}) = \sum_{\sigma} \Phi_{\sigma}^{\dagger}(\mathbf{x}) \left[-\frac{\nabla^2}{2m} - \mu + \mathcal{V}_d(\mathbf{x}) \right] \Phi_{\sigma}(\mathbf{x})$$

$$+ \int dx' \mathcal{V}(\mathbf{x}, \mathbf{x}') \Phi_{\uparrow}^{\dagger}(\mathbf{x}') \Phi_{\downarrow}^{\dagger}(\mathbf{x}) \Phi_{\downarrow}(\mathbf{x}) \Phi_{\uparrow}(\mathbf{x}'), \tag{1}$$

where $\Phi_{\sigma}^{\dagger}(\mathbf{x})$ and $\Phi_{\sigma}(\mathbf{x})$ represent the creation and annihilation of fermions with mass m and spin state σ, respectively at $\mathbf{x}$, $\mathcal{V}_d(\mathbf{x})$ signifies the weak random potential and μ is the chemical potential. We use Planck units, i.e., $\hbar = 1$. In the interaction Hamiltonian the s-wave fermionic interaction is defined as $\mathcal{V}(\mathbf{x}, \mathbf{x}') = -g\delta(\mathbf{x}-\mathbf{x}')$, where g is the bare coupling strength of fermion–fermion pairing which we later regularize through the s-wave scattering length a.

Recent experiments have employed different techniques to create disorder. Most commonly used are laser speckle[7] and quasi-periodic lattice.[8] In our calculation we consider an uncorrelated quenched disorder for simplicity. It implies that the range of the impurities should be much smaller than the average separation between them.

To model it mathematically, we use the pseudo-potential as $\mathcal{V}_d(\mathbf{x}) = \sum_i g_d \delta(\mathbf{x} - \mathbf{x}_i)$, where g_d is the fermionic impurity coupling constant (which is a function of impurity scattering length b), and $\mathbf{x}_i$ are the static positions of the quenched disorder. Thus, the correlation function is $\langle \mathcal{V}_d(-q)\mathcal{V}_d(q) \rangle = \beta \delta_{i\omega_m,0} \gamma$, where $q = (\mathbf{q}, i\omega_m)$. $\beta = 1/k_B T$ is the inverse temperature, $\omega_m = 2\pi m/\beta$ are the bosonic Matsubara frequencies with m an integer. The disorder strength can be written as $\gamma = n_i g_d^2$, where n_i denotes the concentration of the impurities. Simple algebraic manipulations further reveal that γ is a function of the relative size of the impurity (b/a).

The model of disorder described above can be realized in real experiments when a collection of light fermionic species inside a harmonic confinement remains in the same spatial dimension as of the few heavy fermions in an optical lattice. The laser is tuned in such a way that the lighter species cannot see the optical lattice while the heavier species cannot see the parabolic potential.[15]

We use Eq. (1) and the model of disorder, within the modified mean-field formalism through Gaussian fluctuations. After carrying out the self-energy calculation using Dyson equation, effective action can be written as,[13,16]

$$\mathcal{S}_{\text{eff}} = \int d\mathbf{x} \int_0^\beta d\tau \left[\frac{|\Delta(\mathbf{r})|^2}{g} - \frac{1}{\beta} \text{Tr} \ln\{-\beta\mathcal{G}^{-1}(\mathbf{r})\} \right] , \tag{2}$$

where $\mathbf{r} = (\mathbf{x}, \tau)$, $\Delta(\mathbf{r})$ is the pairing gap and $\mathcal{G}^{-1}$ is the inverse Nambu propagator. Expansion of the inverse Nambu propagator up to the second-order, it is possible to write the effective action ($\mathcal{S}_{\text{eff}}$) in Eq. (2) as a sum of bosonic action ($\mathcal{S}_B$) and fermionic action ($\mathcal{S}_F$). There is an additional term which emerges from the linear order of self-energy expansion ($\mathcal{G}_0\Sigma$). It is possible to set the linear order term to zero, if we consider $\mathcal{S}_F$ is an extremum of $\mathcal{S}_{\text{eff}}$, after having performed all the fermionic Matsubara frequency sums. The constrained condition leads to the BCS gap equation, which after appropriate regularization through s-wave scattering length reads,

$$-\frac{m}{4\pi a} = \sum_k \left[\frac{1}{2E_k} - \frac{1}{2\epsilon_k} \right] , \tag{3}$$

where $E_k = \sqrt{\xi_k^2 + \Delta^2}$, $\xi_k = \epsilon_k - \mu$, $\epsilon_k = k^2/(2m)$, μ is the chemical potential and Δ is the BCS gap function. Next we obtain the density equation through the thermodynamic potential (Ω). Ω can be written as a sum over fermionic (Ω_F) and bosonic (Ω_B) potentials, $n = n_F + n_B = -\frac{\partial}{\partial\mu}(\Omega_F + \Omega_B) = -\frac{1}{\beta}\frac{\partial}{\partial\mu}(\mathcal{S}_F + \mathcal{S}_B)$. Hence the mean-field density equation reads

$$n = \sum_k \left(1 - \frac{\xi_k}{E_k} \right) - \frac{\partial\Omega_B}{\partial\mu} , \tag{4}$$

where Ω_B is the bosonic thermodynamic potential which contains the disorder contribution. Now Eqs. (3) and (4) are ready to be solved self-consistently.

2.2. *Fidelity susceptibility*

Study of FS in disordered environment is a subject of interest in recent years, since it offers a unique intrinsic tool to detect QPT.[19–25] A detailed description of QPT in quantum XY model in the presence of disorder has already been reported.[29,30] Furthermore, in a recent analysis the role of FS in a disordered two-dimensional Hubbard model has been considered.[31] Here, we study the FS within the dirty crossover scenario.

The ground-state fidelity $F(\lambda+\delta\lambda, \lambda)$ depends on both the controlling parameter λ and its variation, $\delta\lambda$. The dependence on $\delta\lambda$ can be eliminated by considering the limiting expression for the ground-state fidelity when $\delta\lambda$ approaches zero. For small $\delta\lambda$,

$$F(\lambda + \delta\lambda, \lambda)^2 = \left[\langle\Psi(\lambda)| + \delta\lambda\frac{\partial\langle\Psi(\lambda)|}{\partial\lambda} + \frac{(\delta\lambda)^2}{2}\frac{\partial^2\langle\Psi(\lambda)|}{\partial\lambda^2} \right]|\Psi(\lambda)\rangle$$

$$= 1 - \frac{(\delta\lambda)^2}{2}\frac{\partial\langle\Psi(\lambda)|}{\partial\lambda}\frac{\partial|\Psi(\lambda)\rangle}{\partial\lambda}\,, \tag{5}$$

where the state $|\Psi(\lambda)\rangle$ is assumed to be real and normalized. A sudden drop of the ground-state fidelity at the critical point will then correspond to a divergence of the FS:[20,21]

$$\chi(\lambda) \equiv -\frac{1}{V}\lim_{\delta\lambda\to 0}\frac{4\ln F(\lambda + \delta\lambda, \lambda)}{(\delta\lambda)^2}$$

$$= \frac{1}{V}\frac{\partial\langle\Psi(\lambda)|}{\partial\lambda}\cdot\frac{\partial|\Psi(\lambda)\rangle}{\partial\lambda}\,, \tag{6}$$

where V is the system volume.

Since we are interested in calculating the FS across the BCS–BEC crossover, we calculate $\chi(\lambda)$ for the BCS wavefunction:

$$|\Psi(\lambda)\rangle = \prod_{\mathbf{k}}[u_k(\lambda) + v_k(\lambda)c_{\mathbf{k}\uparrow}^\dagger c_{-\mathbf{k}\downarrow}^\dagger]|0\rangle\,. \tag{7}$$

Here, $c_{\mathbf{k}\sigma}^\dagger$ creates a fermion in the single-particle state of wave-vector $\mathbf{k}$, spin σ and energy ϵ_k, u_k and v_k are the BCS coherence factors, $v_k^2 = 1 - u_k^2 = (1 - \xi_k/E_k)/2$. When the BCS wavefunction is inserted in Eq. (6), one obtains

$$\chi(\lambda) = \int \frac{d\mathbf{k}}{(2\pi)^3}\left[\left(\frac{du_k}{d\lambda}\right)^2 + \left(\frac{dv_k}{d\lambda}\right)^2\right]\,, \tag{8}$$

which can be written as

$$\chi(\lambda) = \int \frac{d\mathbf{k}}{(2\pi)^3}\frac{1}{4E_k^4}\left[\Delta_k\frac{d\mu}{d\lambda} + \xi_k\frac{d\Delta_k}{d\lambda}\right]^2\,. \tag{9}$$

In the numerical calculation of χ, we use the disorder induced self-consistent solution of the order parameter and the chemical potential where $\lambda = (k_F a)^{-1}$.

3. Results and Discussion

We now present our FS results which are obtained through self-consistent calculation of Eqs. (3) and (4) and subsequent numerical integration of Eq. (9). In the first part we show the effect of disorder on FS and related statistical analysis. Afterward we show the effects of disorder on DOS and discuss the possibility of a QPT. Let us now specify what is meant by weak impurity. We know that γ has a dimension of k_F/m^2 which leads to the dimensionless disorder strength $\eta = \gamma m^2/k_F = (3\pi^2/4)\gamma n/\epsilon_F^2$. This implies that the impurity density and strength remains much less than the particle density n and Fermi energy ϵ_F. For practical purposes, one can quantify the impurity contribution as weak, as long as the dimensionless disorder strength satisfies[15] $\eta \lesssim 5$.

3.1. *FS with disorder*

The recent observation of Anderson localization in ultracold atomic gases[7–10] has opened the possibility of studying disorder effects in the whole crossover region. This motivates us to check whether it is possible to predict a QPT in an interaction driven disorder induced ultracold Fermi system. Starting from the clean limit, we increase the impurity strength and observe a gradual change of FS from symmetric to asymmetric profile (Fig. 1). The left panel in Fig. 1 shows FS versus interaction for various disorder strengths ($\eta \in [0,5]$ with increments of 0.2) and the loss of symmetry and decrease of width. The right panel depicts a density plot between interaction, disorder and FS. From this plot one can realize the gradual increase in FS peak height and also a slow shift of the peak to the weaker to relatively stronger coupling. We note that in a study of quantum spin chains similar observations were also made.[30] We thus ask whether this behavior is a precursor of an imminent phase transition with much stronger disorder.[14]

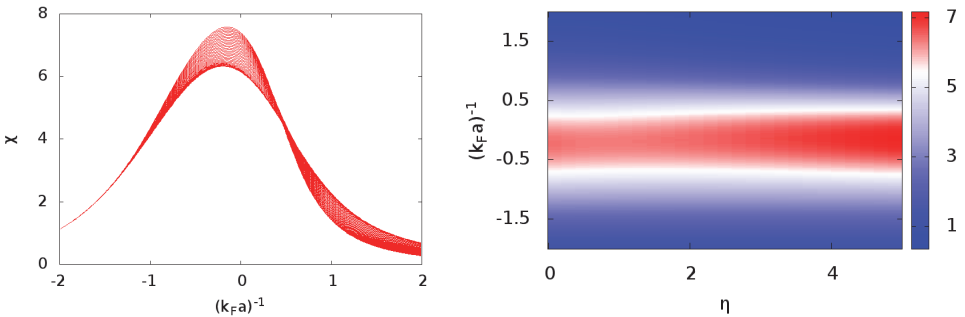

Fig. 1.   (Color online) χ (in units of k_F^{-3}) is plotted for various disorder strengths along the BCS–BEC crossover. The left panel, each χ is separated by an increment of $\eta = 0.2$ from $\eta = 0$ to $\eta = 5$. The behavior reveals the break in symmetry for FS. In the right panel we present the same data in density plot format for a clear understanding of the change in peak height and width of the FS.

A measure of the asymmetry in FS would be a useful tool and thus we calculate the skewness and kurtosis of the FS. In nuclear physics skewness and kurtosis are established tools to study the phase transition from an equilibrium hadronic state to quark-gluon plasma.[32,33] Furthermore, these techniques are also applicable to chiral phase transition in quantum chromodynamics (QCD).[34] Skewness (S) is defined as the measure of the asymmetry of the distribution, and kurtosis (κ) measures the curvature of the distribution peak, which are defined as

$$S = \frac{\langle (x - \langle x \rangle)^3 \rangle}{\langle (x - \langle x \rangle)^2 \rangle^{3/2}}, \quad \kappa = \frac{\langle (x - \langle x \rangle)^4 \rangle}{\langle (x - \langle x \rangle)^2 \rangle^2} - 3 \,. \tag{10}$$

In the present context $x = (k_F a)^{-1}$. The critical transition point can be identified as the point where S and κ change sign, since the change of sign will signify an abrupt nonanalytic change in the orientation (for skewness) and height (for kurtosis) of the distribution. Hence, they can be used as indicators of an impending transition.

Physically, the change of sign in skewness can be viewed as change of direction of asymmetry from left to right or vice versa. In the case of κ it can be viewed as change of a sharp distribution to a flat one. At the phase transition, FS is expected to diverge as a result of a sudden drop in fidelity.[27] Here, we expect that, as we near the transition point the FS distribution should become increasingly sharper resulting in an increasingly larger kurtosis.

We calculate S and κ as a function of disorder which are depicted in Fig. 2. In this figure, the left panel represents the skewness, which being positive implies that the FS distribution tail is longer on the BEC side. The right panel tells us about the kurtosis which is negative, and thus corresponds to a flatter peak which is usually observed in the phase transition.[33] The solid line depicts the calculated S and κ. The bold points are our nonlinear extrapolation of the data.

We observe, with increasing disorder, the FS peak moves towards the relatively strong interaction regime and the asymmetry gradually increases which can be viewed in the progressive change of S and κ in Fig. 2. From the Anderson theorem it is known that in three-dimensions there exits a critical impurity strength beyond
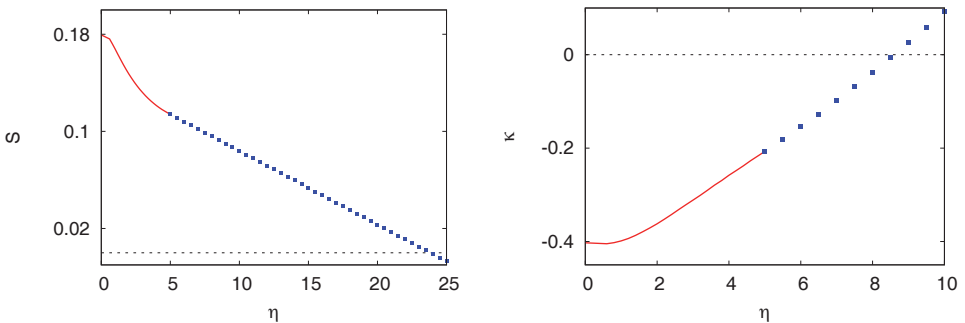

Fig. 2. (Color online) The left panel presents the skewness whereas the lower panel is the kurtosis. Our calculation of skewness and kurtosis are presented through the solid line. The bold points depict the nonlinear extrapolation and the dotted line indicates the zero axis.

which the electrons will be localized. In this study, we cannot comment exactly on the localization because of the limitations of the modified mean-field theory. However, it can be noticed (Fig. 2) that both S and κ approach zero where a sign change will occur (possible phase transition). To estimate the critical point of phase transition, we first apply least square fitting of the data points which indicates that η_c is around $10 - 13$. As an alternative, we also employ nonlinear spline interpolation. The results suggest the zero crossing for these moments may occur at $\eta_c \simeq 9$ (kurtosis) and $\eta_c \simeq 23$ (skewness). A range of values for η_c in S and κ has also been encountered in the study of quark-gluon plasma with the suggested interpretation of $\eta_c \simeq 9$ signifying the beginning of the QPT and $\eta_c \simeq 23$ indicating the completion of QPT.[33] We also note that our linearly extrapolated critical point is in agreement with Ref. 14, where η_c is estimated to be around 11.

3.2. *DOS with disorder*

In the previous section we have considered the possibility of a QPT in a dirty crossover. To study the influence of disorder in the BCS–BEC crossover more closely, we calculate the DOS defined as

$$N(\omega) = \sum_k u_k^2 \delta(\omega - E_k) + v_k^2 \delta(\omega + E_k) \,, \tag{11}$$

where u_k, v_k and E_k are the usual BCS parameters as introduced earlier.

In Fig. 3 we present the behavior of DOS, $N(\omega)$, at different interaction regimes. Interestingly, we do not observe any significant difference in BCS and BEC limit in terms of energy gap as well as stacking of energy states. But at unitarity, the
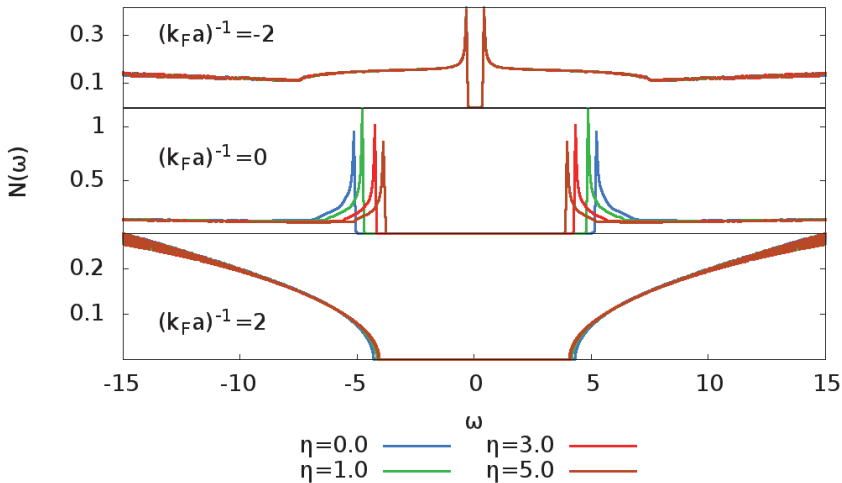

Fig. 3. (Color online) The DOS for different couplings and various disorder strengths is presented. From top to bottom the figures describe weak coupling, unitarity and strong coupling regions respectively. It is noticeable that disorder plays a significant part only in the unitarity leaving the other two regions almost unchanged.
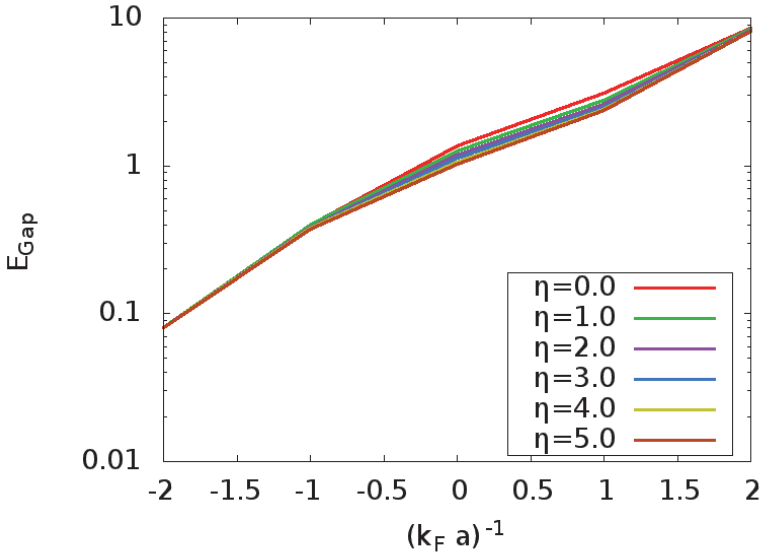
Fig. 4. (Color online) Variation of the energy gap (spectral gap) with disorder strength and interaction energy is shown. A distinct drop in E_{Gap} can be noted in the crossover region due to disorder and this drop increases with increasing impurity strength. However the two extremes (BCS and BEC) do not show much change.

energy gap gradually reduces as a function of disorder and sharp coherence peaks at the excitation edges are observed.

We examine this behavior more closely in Fig. 4. In the BCS–BEC crossover region ($(k_F a)^{-1} \in [-1, 1]$) one can observe that the E_{Gap} is reduced, but on the BCS and BEC sides it remains unaffected by disorder. It is interesting to note that in a recent study on coexistence of pseudogap and usual BCS energy gap in a harmonic trap,[36] the reduction of energy gap was observed only at unitarity when the DOS was calculated at different positions from trap center. We already know that in a BCS superconductor the energy gap reduces at moderate disorder but starts increasing for stronger disorder, which brings the onset of localization. Here the effect of disorder is more prevalent at unitarity compared to the other regions. This can be taken as an indication of an early onset of QPT at unitarity and the emergence of a transient state (glassy phase) at relatively moderate disorder.

3.3. *Discussion*

In this work we have combined different ideas from condensed matter physics and quantum information theory to investigate the effect of disorder on the BCS–BEC crossover. We now discus various aspects and experimental perspectives of the ideas presented here.

We emphasize that through a relatively simple method we are able to comment on the possible QPT in a disordered unitary Fermi gas. Apart from a detailed

real space analysis of the inhomogeneous system (by employing a BdG analysis) it will also be very interesting to see the effect of the impurity in this model by incorporating higher-orders in the Dyson equation. Such a comparative study, involving the third- and fourth-orders in the free energy expansion would be useful in understanding the range of validity of the perturbation theory.

We note that Bose gas experiments were conducted with different disorder realizations such as speckle and incommensurate (bichromatic) lattice.[7,8] To realize the proper range of localization length (smaller than the system size) it is necessary to design an appropriate optical system for speckle potential. However, the quasiperiodic lattice naturally provides a very short coherence length.[38] The uneven landscape of the impurity potential allows existence of spatially confined states which can result in "island" formation of superfluid system in an otherwise insulating domain and this feature is expected to influence the Bose condensate more severely than the BCS Cooper pairs because of strong phase coherence. The quenched disorder described here is repulsive, thus it is nonconfining. The impurity potential represents essentially the scattering centers which affect mostly the phases of the wavefunctions of the particles that are scattered from them. Thus, the model does not influence any localization inherently.

We also note that the use of FS is gathering attention in the study of ultracold atomic systems.[39] From the quantum information theory side, an experimental model to observe fidelity was suggested almost a decade ago[40] and it is observed in photon entanglement measurements.[41] Since one can now observe the macroscopic wavefunctions in ultracold atom experiments, we expect the realization of the overlap of two wavefunctions in the near future.

4. Conclusion

In conclusion, we have considered the possibility of QPT near unitarity through the study of FS and DOS with quenched disorder. The disorder is included in the mean-field formalism through Gaussian fluctuations. The FS provides a strong indication in terms of evolution from symmetric to asymmetric FS line-shape due to disorder for a QPT. A more detailed real space analysis with strong disorder should provide further information on this issue.

We have calculated the DOS for different interaction regimes. Interestingly, the DOS shows sharp coherence peaks at the excitation edges and gradual lowering of the energy gap. On the other hand, the DOS remains almost the same as that of a clean system in the deep BCS and BEC regimes. This suggests that the unitary superfluid is a better candidate for impending disorder driven QPT.

We note that the effect of impurities in superconducting lattice systems has been extensively studied. The emergence of ultracold Fermi gases necessitates a detailed investigation with disorder in a homogeneous continuum model. The quenched disorder model within the BEC has been studied through the mean-field theory and QMC simulations.[35,42,43] A systematic description across the crossover is missing.

We hope our analysis will bridge this gap and stimulate further investigations in the whole crossover.

Acknowledgment

References

1. C. Chin *et al.*, *Rev. Mod. Phys.* **82**, 1225 (2010).
2. S. Georgini, L. P. Pitaevskii and S. Stringari, *Rev. Mod. Phys.* **80**, 1215 (2008).
3. I. Bloch, J. Dalibard and W. Zwerger, *Rev. Mod. Phys.* **80**, 885 (2008).
4. L. He, S. Mao and P. Zhuang, *Int. J. Mod. Phys. A* **28**, 1330054 (2013).
5. P. W. Anderson, *J. Phys. Chem. Solids* **11**, 26 (1959).
6. V. A. Alekseev *et al.*, *JETP Lett.* **24**, 189 (1976).
7. J. Billy *et al.*, *Nature* **453**, 891 (2008).
8. G. Roati *et al.*, *Nature* **453**, 895 (2008).
9. S. S. Kondov *et al.*, *Science* **334**, 66 (2011).
10. F. Jendrzejewski *et al.*, *Nat. Phys.* **8**, 398 (2012).
11. L. S. Palencia and M. Lewenstein, *Nat. Phys.* **6**, 87 (2010).
12. P. Dey and S. Basu, *J. Phys. Cond. Mat.* **20**, 485205 (2008).
13. G. Orso, *Phys. Rev. Lett.* **99**. 250402 (2007).
14. L. Han and C. A. R. Sá de Melo, arXiv:0904.4197.
15. L. Han and C. A. R. Sá de Melo, *New J. Phys.* **13**, 055012 (2011).
16. A. Khan, S. Basu and S. W. Kim, *J. Phys. B: At. Mol. Opt. Phys.* **45**, 135302 (2012).
17. A. Khan, *Int. J. Mod. Phys. Conf. Ser.* **11**, 120 (2012).
18. L. Pollet *et al.*, *Phys. Rev. Lett.* **103**, 140402 (2009).
19. P. Zanardi and N. Paunković, *Phys. Rev. E* **74**, 031123 (2006).
20. W. L. You, Y. W. Li and S. J. Gu, *Phys. Rev. E* **76**, 022101 (2007).
21. M. F. Yang, *Phys. Rev. B* **76**, 180403(R) (2007).
22. S. Chen *et al.*, *Phys. Rev. E* **76**, 061108 (2007).
23. L. Campos Venuti and P. Zanardi, *Phys. Rev. Lett.* **99**, 095701 (2007).
24. P. Zanardi, P. Giorda and M. Cozzini, *Phys. Rev. Lett.* **99**, 100603 (2007).
25. P. Buonsante and A. Vezzani, *Phys. Rev. Lett.* **98**, 110601 (2007).
26. S. J. Gu, *Int. J. Mod. Phys. B* **24**, 4371 (2010).
27. A. Khan and P. Pieri, *Phys. Rev. A* **80** 012303 (2009).
28. A. Ghoshal, M. Randeria and N. Trivedi, *Phys. Rev. B* **65** 014501 (2001).
29. S. Garnerone *et al.*, *Phys. Rev. Lett.* **102**, 057205 (2009).
30. N. T. Jacobson *et al.*, *Phys. Rev. B* **79**, 184427 (2009).
31. P. Dey *et al.*, *Eur. Phys. J. B* **81**, 95 (2011).
32. B. Müller, *Science* **332**, 1513 (2011).
33. L. P. Csernai, G. Mocanu and Z. Néda, *Phys. Rev. C* **85**, 068201 (2012).
34. B. Stokić, B. Friman and K. Redlichb, *Phys. Lett. B* **673**, 192 (2009).
35. G. E. Astrakharchik *et al.*, *Phys. Rev. A* **66**, 023603 (2002).
36. R. Watanabe, S. Tsuchiya and Y. Ohashi, *Phys. Rev. A* **86**, 063603 (2012).
37. A. Mielke, *J. Phys. Cond. Mat.* **2**, 9567 (1990).

38. G. Modugno, *Rep. Prog. Phys.* **73**, 102401 (2010).
39. J. Carrasquilla, S. R. Manmana and M. Rigol, *Phys. Rev. A* **87**, 043606 (2013).
40. A. K. Ekert *et al.*, *Phys. Rev. Lett.* **88**, 217901 (2002).
41. N. Kiesel *et al.*, *Phys. Rev. Lett.* **98**, 063604 (2007).
42. K. Huang and H. F. Meng, *Phys. Rev. Lett.* **69**, 644 (1992).
43. S. Giorgini, L. Pitaevskii and S. Stringari, *Phys. Rev. B* **49**, 12938 (1994).